Int J Clin Exp Pathol 2018;11(2):650-663
www.ijcep.com /ISSN:1936-2625/IJCEP0069558

Original Article

Plasma CAMK2A predicts chemotherapy resistance in metastatic triple negative breast cancer

Bin Shao[1*], Zhihua Tian[2*], Huirong Ding[2*], Qingsong Wang[3], Guohong Song[1], Lijun Di[1], Hong Zhang[2], Huiping Li[1], Jing Shen[2]

Key Laboratory of Carcinogenesis and Translational Research (Ministry of Education/Beijing), [1]Department of Medical Oncology, [2]Central Laboratory, Peking University Cancer Hospital & Institute, Beijing, P. R. China; [3]State Key Laboratory of Protein and Plant Gene Research, College of Life Sciences, Peking University, Beijing, P. R. China. [*]Equal contributors.

Received November 21, 2017; Accepted December 15, 2017; Epub February 1, 2018; Published February 15, 2018

Abstract: Background: Chemotherapy resistance is a great obstacle in effective treatment for metastatic triple negative breast cancer (TNBC). The ability to predict chemotherapy response would allow chemotherapy administration to be directed toward only those patients who would benefit, thus maximizing treatment efficiency. Differentially expressed plasma proteins may serve as putative biomarkers for predicting chemotherapy outcomes. Patients and methods: In this study, 26 plasma samples (10 samples with partial response (S) and 16 samples with progression disease (R)) from patients with metastatic TNBC were measured by Tandem Mass Tag (TMT)-based proteomics analysis to identify differentially expressed proteins between the S and R group. Potential proteinswere validated with enzyme-linked immunosorbent assay (ELISA) in another 67 plasma samples. Results: A total of 320 plasma proteins were identified, and statistical analysis showed that 108 proteins were significantly dysregulated between R and S groups in the screening stage. Bioinformatics revealed relevant pathways and regulatory networks of the differentially expressed proteins. Three differentially expressed proteins were validated by ELISA with 67 samples from TNBC patients. The R group had significantly higher plasma CAMK2A level than the S group (P=0.0074). The ROC curve analysis showed an AUC of 0.708, with sensitivity 48.4% and specificity 86.1%. In multivariate logistic regression analysis, the level of plasma CAMK2A was also significant for chemotherapeutic response (P=0.009, OR=0.152). Furthermore, the patients with higher CAMK2A level had shorter OS than those with lower CAMK2A level, which amounted to 13.9 and 28.9 months, respectively (P=0.034). In the multivariate Cox regression analysis, CAMK2A level still had significant effect on OS (P=0.031, HR=1.865). Conclusion: TMT-based proteomic analysis was able to identify potential biomarkers in plasma that predicted chemotherapy resistance in the metastatic TNBC. The plasma of CAMK2A level may serve as apotential predictive and prognostic biomarker for chemotherapy in metastatic TNBC.

Keywords: Triple negative breast cancer, tandem mass tag, proteomics, plasma, biomarkers

Introduction

Breast cancer is the most common disease and the second leading cause of women death worldwide [1]. In China, the incidence has increased significantly [2]. 30% of early-stage breast cancer developed with metastasis, and about 5% of patients are diagnosed with advanced stage with distant metastasis [3]. Improvements of treatment did not change the prognosis of metastatic breast cancer. The 5-year survival rate of metastatic breast cancer is only 23%, which is much lower than 84-99% in early-stage breast cancer [4].

Around 15-20% of breast cancer cases are classifiedas triple-negative breast cancer (TNBC), named afterthe absence of the expression of estrogen receptor (ER), progesterone receptor (PR), and human epidermal growth factor receptor 2 (HER2). Patients with TNBC suffer from poor clinical outcome and shortage of targeted therapy. Chemotherapy plays an important role in the treatment paradigms for metastatic TNBC. Docetaxel is a classical drug for metastatic TNBC. However, chemotherapy resistance will ultimately be developed which impedes the success of chemotherapy. Plasma serves as an important medium that interacts

Table 1. Clinicopathological characteristics of the metastatic breast cancer

Characteristics	Screening stage n=26 (%)	Validation stage n=67 (%)
Age (years) median (range)	55 (35-72)	53 (30-80)
ECOG		
0, 1	25 (96.2)	63 (94.0)
2	1 (3.8)	4 (6.0)
Histology		
IDC	25 (96.2)	58 (86.5)
ILC	1 (3.8)	3 (4.5)
Others	0	6 (9.0)
Histologic grading		
Grade 1	7 (35)	24 (35.8)
Grade 2	8 (40)	31 (46.3)
Grade 3	5 (25)	12 (17.9)
AJCC stage		
Stage I	1 (3.8)	4 (6.0)
Stage II	12 (46.2)	30 (44.8)
Stage III	8 (30.8)	24 (35.8)
Stage IV	3 (11.5)	5 (7.5)
Unknown	2 (7.7)	4 (6.0)
Internalorgan metastasis (liver, lung, brain)	14 (53.8)	32 (47.8)
More than 2 sites of metastasis	12 (46.2)	28 (41.8)
Clinical response		
PR	10 (38.5)	33 (49.3)
PD	16 (61.5)	34 (50.7)
PFS (months)	3.2 (2.9-3.6)	5.1 (2.0-8.2)
OS (months)	21.0 (14.1-28.0)	18.1 (10.3-25.8)

Note: ECOG: Eastern Cooperative Oncology Group; IDC: Invasive ductal carcinoma; ILC: Invasive lobular carcinoma; PR: Partial response; PD: Progression disease; PFS: Progression free survival; OS: Overall survival.

with cells, tissues and organs in the human body. It carries proteins secreted or leaked by different cells in response to pathologic progress. The serum and plasma proteins or peptides have been shown to be good biomarkers for early diagnosis, prognosis, and metastasis in breast cancer [5-7]. Therefore, identification of differentially expressed plasma proteins might offer a rich source of information for development of biomarkers that predictdocetaxel-based chemotherapy resistance from metastatic TNBC patients [8, 9]. To date, proteomic technology has been applied to a wide range of cancer studies including analysis of drug resistance [10]. Mass spectrometry (MS)-based proteomics often involves analyzing complex mixtures of proteins derived from cell or tissue lysates or from body fluids on a global scale [11-13]. To our knowledge, no study has been performed to search docetaxel-based chemotherapy resistant markers on plasma samples from metastatic TNBC patients.

In the present study, we applied Tandem Mass Tag (TMT)-based quantitative mass spectrometry to distinguish the differentially expressed proteins between the chemotherapy-sensitive and chemotherapy-resistant plasma from metastatic TNBC patients. The dataset was analyzed using the DAVID and STRING databases, and differentially expressed proteins were further validated by enzyme-linked immunosorbent assay (ELISA). The aim of the study was to identify differences in protein expression to give further insight into the molecular mechanisms on chemotherapy resistance. The association between differentially expressed proteins level and patient survival was also investigated to determine its potential prognostic utility.

Materialsand methods

Patients

The study was approved by the Ethics Committee of the Peking University Cancer Hospital on 12-Dec-2014 and conforms to the principles outlined in the Declaration of Helsinki. Informed consent was obtained from each patient. The plasma of patients with metastatic TNBC was sampled between June 2009 and Dec 2013 from the specimen bank of Beijing Cancer Hospital. The estrogen receptor (ER), progesterone receptor (PR), and HER2 status were the result of the primary tumor. ER and PR status

were considered positive when 1% or more tumor cells exhibited nuclear staining for these receptors. HER2 positivity was defined as either as score of 3^+ by immunohistochemistry (IHC) or positivity by FISH. All the patients received docetaxel (75 mg/m^2 every 21 days for 4-6 cycles) based chemotherapy. Treatment response was assessed after two cycles of chemotherapy by the RECIST criteria 1.1. Patients achieving partial response (PR) were considered aschemotherapy-sensitive (S) group. Patients achieving disease progression (PD) were considered aschemotherapy-resistant (R) group. Demographic and clinicopathologic details of patients were obtained from the medical records of the Department of Breast Oncology (**Table 1**). Patients with underlying-medical conditions that could result in systematic alterationin plasma protein levels were excluded. Exclusion conditions included systemic lupus, rheumatoid arthritis, scleroderma, polymyositis, chronic liver disease, chronic renal failure, and diabetes mellitus.

Plasma samples

Four milliliters of peripheral blood were collected before chemotherapy. Blood was collected in EDTA-containing tubes (BD Diagnostics, La Jolla, CA) and centrifuged at 2000 rpm for 15 min within 1 h of collection to remove cellular components. Plasma samples were divided into aliquots and stored at -80°C until use. Specimens showing hemolysis were excluded.

Protein tryptic digestion

Theplasma samples were diluted 10-fold with 50 mM NH_4HCO_3 pH 8.5. The diluted plasma protein concentrations were measured by the BCA Protein Assay Kit (Thermo Fisher Scientific). Proteins were reduced with 5 mM dithiothreitol for 30 min at 37°C, andalkylated with 15 mM iodoacetamide for 40 min at room temperaturein the dark. Protein samples were digested with sequencing grade modified trypsin (Promega) (ratio of trypsin to protein 1:50) at 37°C overnight. Digests were acidified by addition of 10% trifluoroacetic acid (TFA) to 0.5% finalconcentration and the peptides were desalted on Sep-Pak tC18 cartridges (Waters, Milford, MA, USA) and concentrated in a centrifugal evaporator (Thermo Fisher Scientific).

Peptide TMT labeling

Fifty micrograms of digested peptides from each sample group were used for amine-reactive TMT6-plex labelingaccording to themanufacturer's protocol (Thermo Fisher Scientific, USA). Briefly, peptides were resuspended in 100 µl of 0.1 M TEAB buffer pH 8.5 and were labeled with TMT6-plex tags which were dissolved in 41 µl of anhydrous acetonitrile (ACN) and added to each sample with briefly mixing. Reactions were incubated at RTfor 1 h, and then quenched by the addition of 10 µl of 5% hydroxylamine for 15 min and then acidified by the addition of 10 µl 100% formic acid. Each TMT-labeled samplewas mixed equally and the mixed peptides were desalted with Sep-Pak C18 cartridges.

Isoelectric focusing fractionation of TMT-labeled peptides

For TMT-labeled samples, 200 µg peptide mixtures were dissolved in buffer containing 5% glycerol and 2% immobilized pH gradient buffer (pH 3-10; GE Healthcare) and loaded into 24 wells over an Immobiline DryStrip (24 cm, pH 3-10; GE Healthcare). The peptide mixtures were fractionated by peptide IEF on a 3100 OFFGEL fractionator (Agilent Technologies) according to the manufacturer's instructions. A total of 24 fractions were acidified and desalted with C18 Stagetips. The eluted peptides were dried in a vacuum centrifuge.

LC-MS/MS analysis

All experiments were performed using an EASY-nLC 1000 ultra-high pressure system (Thermo Fisher Scientific) coupled to a LTQ Orbitrap XL mass spectrometer (Thermo Fisher Scientific) according to a previous report [11, 12]. Briefly, TMT labeled peptides were separated on 15 cm in-house packed HPLC-columns (100 µmi.d., 360 µmo.d.) with ReproSil-Pur C18-AQ 3 µm resin by Dr. Maisch GmbH. For all measurements, peptides were loaded in buffer A (0.1% formic acid) and eluted with a linear 100 min gradient of 5-30% of buffer B (0.1% formic acid, 100% acetonitrile). The flow rate was kept at 300 nL/min. Mass spectrometry instrument methods for TMT-labeled sample analysis consisted of MS1 survey scans (1×10^6 target value; 30,000 resolution; 300-1,600 Th). The MS/MS spectra of the 3 most intense ions

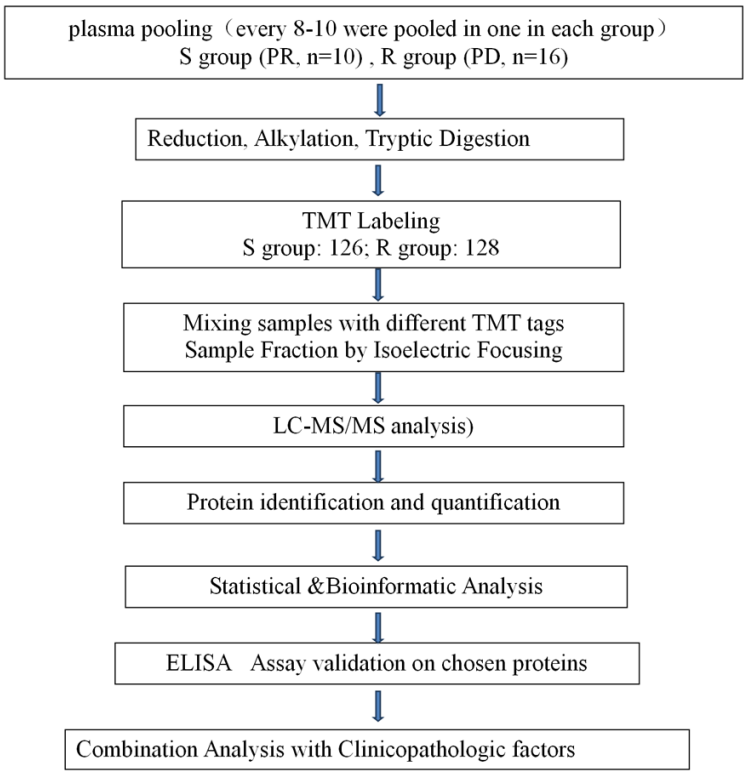

Figure 1. General workflow of the present study. Of a total of 67 plasma samples, 26 samples was used in the screening stage, every 10-16 plasmas in the same group were pooled into one sample. A TMT-based quantitative proteomics analysis for plasma was used to gain a global view of proteome profiling to different responses of docetaxel-based chemotherapy.

were acquired by higher-energy c-trap dissociation (HCD, normalized collision energy, 70%; activation time, 40 ms) in the Orbitrap at a mass resolution of 7500, and collision induced dissociation (CID, normalized collision energy, 35%; activation time, 30 ms) in the ion trap. Dynamic exclusion duration was set to 30 s with a maximum exclusion list of 500. The data were acquired using Xcalibur 2.2 (Thermo Fisher Scientific).

Protein identification and quantification

TMT data sets were processed separately using the Proteome discoverer software (Version 1.4, Thermo Fisher Scientific). Searches were performed against a non-redundant concatenated human database protein sequence database (UniProt, 2014. 12. 18) containing both forward and reverse protein sequences. The search parameters were as follows: trypsin as the digesting enzyme; 2 miscleavages allowed; carbamidomethylation (C) as the fixed modification; oxidation (M) and TMT6-plex labels at the lysine residues and N-terminus as variable modifications; 10 ppm for MS tolerance; and 0.5 Da for MS/MS tolerance. The false discovery rate for peptides and proteins was set at 0.01, and at least one unique peptide was required for protein identification.

Bioinformatic analysis

The differentially expressed proteins were entered into the DAVID database for functional analysis. Protein-protein interaction (PPI) networks construction and KEGG pathway enrichment analysis were performed using the STRING database (Search Tool for the Retrieval of Interacting Genes/Proteins, Version 10.5) at the website: http://string-db.org/.

ELISA validation

An ELISA assay was applied to validate changes of selected proteins to confirm the TMT proteomics results. Human CAMK2A and CKB ELISA Kit were purchased from LifeSpan Biosciences (USA); 14-3-3 Gamma ELISA Kit was purchased from MBL Life Science (Japan). All ELISA assays were performed according to manufacturer's protocols.

Statistical analysis

Patients' demographic and clinicopathologic characteristics were summarized through descriptive analysis. Continuous variables were reported through median and range, whereas categorical variables were described through frequency distributionPFS and OS curves and were calculated by the Kaplan-Meier method and compared by the log rank test. Multivariate Cox regression analysis was used to estimate hazard ratios for PFS and OS. All statistics were calculated using statistical package for the social sciences (SPSS) 18.0 software. $P<0.05$ was considered to indicate a statistically significant difference. For the discovery stage a 1.3-fold change was used as a combined threshold to define biologically regulated proteins.

Table 2. Summary of the proteins identified as differentially expressed using the TMT-based quantitative proteomics approach

Accession No.	Gene Name	Protein Name	Ratio (R/S)
P67936	TPM4	Tropomyosin alpha-4 chain	0.186
H3BT58	COTL1	Coactosin-like protein	0.274
Q5TCU6	TLN1	Talin-1 OS=Homo sapiens	0.348
K7EJ44	PFN1	Profilin-1	0.354
P05060	CHGB	Secretogranin-1	0.453
Q92496-2	CFHR4	Complement factor H-related protein 4	0.509
P11226	MBL2	Mannose-binding protein C	0.549
P04275	VWF	Von Willebrand factor	0.578
P02776	PF4	Platelet factor 4	0.582
Q9NU22	MDN1	Midasin	0.584
Q96IY4-2	CPB2	Carboxypeptidase B2	0.591
P02679-2	FGG	Fibrinogen gamma chain	0.605
Q6UY14-2	ADAMTSL4	ADAMTS-like protein 4	0.636
P62937	PPIA	Peptidyl-prolyl cis-trans isomerase A	0.640
E7EUV1	MUC2	Mucin-2	0.655
C9JEV0	AZGP1	Zinc-alpha-2-glycoprotein	0.658
E9PQD6	SAA1	Serum amyloid A protein	0.665
P01833	PIGR	Polymeric immunoglobulin receptor	0.679
Q04756	HGFAC	Hepatocyte growth factor activator	0.680
P02675	FGB	Fibrinogen beta chain	0.682
P14151	SELL	L-selectin	0.687
K7ERI9	APOC1	Apolipoprotein C-I, basic form	0.692
E9PKC6	CD44	CD44 antigen	0.700
P02671	FGA	Fibrinogen alpha chain	0.709
P02763	ORM1	Alpha-1-acid glycoprotein 1	0.710
P02743	APCS	Serum amyloid P-component	0.720
F5H5I5	ABCB9	ATP-binding cassette sub-family B member 9	0.738
P05090	APOD	Apolipoprotein D	0.741
P55056	APOC4	Apolipoprotein C-IV	0.742
P04211	IGLV7-43	Ig lambda chain V region 4A	0.744
R4GMN9	NCAM1	Neural cell adhesion molecule 1	0.744
Q13131-2	PRKAA1	5'-AMP-activated protein kinase catalytic subunit alpha-1	0.747
O95445-2	APOM	Apolipoprotein M	0.749
B4DJK0	SRSF5	Serine/arginine-rich splicing factor 5	0.751
P0C0L5	C4B	Complement C4-B	0.754
I3L1J1	SHBG	Sex hormone-binding globulin	0.755
P01008	SERPINC1	Antithrombin-III	0.756
Q9Y6R7	FCGBP	IgGFc-binding protein	0.756
P01042	KNG1	Kininogen-1	0.766
P0CG05	IGLC2	Ig lambda-2 chain C regions	0.766
P69905	HBA1	Hemoglobin subunit alpha	0.766
P55072	VCP	Transitional endoplasmic reticulum ATPase	0.768
P68871	HBB	Hemoglobin subunit beta	0.769
Q16352	INA	Alpha-internexin	1.316
Q92777-2	SYN2	Isoform IIb of Synapsin-2	1.321
P18135	IGKV3-20	Ig kappa chain V-III region HAH	1.321

P07196	NEFL	Neurofilament light polypeptide	1.323
Q16555-2	DPYSL2	Isoform 2 of Dihydropyrimidinase-related protein 2	1.329
P62328	TMSB4X	Thymosin beta-4	1.337
P01877	IGHA2	Ig alpha-2 chain C region	1.348
P25705-2	ATP5A1	Isoform 2 of ATP synthase subunit alpha, mitochondrial	1.351
C9JPG5	SEMA3F	Semaphorin-3F	1.377
P98160	HSPG2	Basement membrane-specific heparan sulfate proteoglycan core protein	1.379
E2QRF9	GMNN	Geminin	1.382
P01608	IGKV1D-33	Ig kappa chain V-I region Roy	1.389
P61026	RAB10	Ras-related protein Rab-10	1.392
P40197	GP5	Platelet glycoprotein V	1.408
P08519	LPA	Apolipoprotein(a)	1.408
M0R1V7	UBA52	Ubiquitin-60S ribosomal protein L40	1.422
P01857	IGHG1	Ig gamma-1 chain C region	1.429
P23083	IGHV1-2	Ig heavy chain V-I region V35	1.442
M0R116	ATP1A3	Sodium/potassium-transporting ATPase subunit alpha-3	1.468
Q01082-3	SPTBN1	Spectrin beta chain	1.475
H7C2G3	C21orf33	ES1 protein homolog, mitochondrial (Fragment)	1.510
Q13509	TUBB3	Tubulin beta-3 chain	1.528
B8ZZ54	HSPE1	10 kDa heat shock protein, mitochondrial	1.531
P08238	HSP90AB1	Heat shock protein HSP 90-beta	1.532
P68366-2	TUBA4A	Isoform 2 of Tubulin alpha-4A chain	1.536
E9PKE3	HSPA8	Heat shock cognate 71 kDa protein	1.557
Q08380	LGALS3BP	Galectin-3-binding protein	1.558
P06753-7	TPM3	Tropomyosin alpha-3 chain	1.563
B7Z1R5	ATP6V1A	V-type proton ATPase catalytic subunit A	1.567
Q13813-2	SPTAN1	Isoform 2 of Spectrin alpha chain, non-erythrocytic 1	1.568
Q13885	TUBB2A	Tubulin beta-2A chain	1.574
P62158	CALM1	Calmodulin	1.604
H3BQ34	PKM	Pyruvate kinase	1.607
Q99798	ACO2	Aconitate hydratase, mitochondrial	1.623
P63104	YWHAZ	14-3-3 protein zeta/delta	1.630
E9PMR5	MBP	Myelin basic protein	1.630
H3BMQ8	ALDOA	Fructose-bisphosphate aldolase A	1.637
P61981	YWHAG	14-3-3 protein gamma	1.637
P04271	S100B	Protein S100-B	1.702
I7HJJ0	SLC25A6	ADP/ATP translocase 3 (Fragment)	1.702
Q71U36-2	TUBA1A	Isoform 2 of Tubulin alpha-1A chain	1.703
K7EKU0	GPATCH8	G patch domain-containing protein 8	1.721
H7BZC1	HPCAL1	Hippocalcin-like protein 1	1.729
K7EKH6	GFAP	Glial fibrillary acidic protein	1.740
B7Z2X9	ENO2	Gamma-enolase	1.744
P01861	IGHG4	Ig gamma-4 chain C region	1.751
O95236-3	APOL3	Apolipoprotein L3	1.774
D6REX5	SEPP1	Selenoprotein P (Fragment)	1.803
P27348	YWHAQ	14-3-3 protein theta	1.816
F5H5G7	LDHC	L-lactate dehydrogenase	1.816
C9JZ20	PHB	Prohibitin	1.838
Q8NEX6	WFDC11	Protein WFDC11	1.887

P12277	CKB	Creatine kinase B-type	1.916
U3KPZ0	TPI1	Triosephosphate isomerase	1.965
D6R9Z7	COX7C	Cytochrome c oxidase subunit 7C, mitochondrial	1.981
H7C394	CAMK2B	Calcium/calmodulin-dependent protein kinase type II subunit beta	2.078
Q00610-2	CLTC	Isoform 2 of Clathrin heavy chain 1	2.125
O43423	ANP32C	Acidic leucine-rich nuclear phosphoprotein 32 family member C	2.141
Q9UQM7	CAMK2A	Calcium/calmodulin-dependent protein kinase type II subunit alpha	2.170
B1AKQ8	GNB1	Guanine nucleotide-binding protein G(I)/G(S)/G(T) subunit beta-1	2.451
P62258	YWHAE	14-3-3 protein epsilon	2.479
P15104	GLUL	Glutamine synthetase	3.370
E5RJH4	PPP3CC	Serine/threonine-protein phosphatase 2B catalytic subunit gamma isoform	3.768
K7EKH5	ALDOC	Fructose-bisphosphate aldolase C (Fragment)	4.683
P62805	HIST1H4A	Histone H4	5.765

Results

Analytical strategy for plasma proteome identification with different docetaxel-based chemotherapy responses

The analytical strategy of the TMT-based quantitative proteomics approach used in the study is shown in **Figure 1**. It was divided into two main stages. First was the biomarker discovery stage consisting of plasma sample preparation, protein expression analysis, and bioinformatics analysis (PPI, GO and KEGG); the second stage was the validation stage consisting of ELISA assay validation and combination analysis with clinicopathologic factors.

Plasma protein expression analysis

A total of 320 non-redundant proteins were identified. Proteins with more than 1.3-fold changes were considered as adifferentially expressed protein. We found a total of 108 significantly dysregulated proteins, among which 65 were up-regulated and 43 were down-regulated in the R group. The details of the 108 proteins, including Uniprotprotein ID, gene name, protein name, ratio (R/S) are listed in **Table 2**.

Functional classification and protein-protein interaction analysis of differentially expressed proteins

To analyze the function of proteins, a protein-protein interaction network was constructed for 108 differentially expressed proteins by retrieving the known interactions between each protein (**Figure 2**). The 108 significantly dysregulated proteins were then interrogated and mapped to KEGG pathways (**Table 3**), and the three significantly enriched pathways were complement and coagulation cascades, biosynthesis of amino acids, and oocyte meiosis. To further extend our knowledge about the change of plasma proteins between R and S groups, GO analysis was performed to reveal the molecular function, biological process, and cellular component associated with the 108 significantly differentially expressed proteins. As shown in **Table 3**, the significantly regulated proteins were highly correlated with regulation of biological quality, platelet degranulation and activation, response to wounding etc. In terms of biological process, they were highly correlated with participating in the processes of protein binding, structural constituents of the cytoskeleton and carbohydrate derivative binding etc. In terms of molecular function, they were highly correlated with the extracellular region and vesicles.

Validation of differential expression of proteins

A total of 67 samples were recruited for ELISA analysis to validate the protein level of CAMK2A (Calcium/calmodulin-dependent protein kinase type II subunit alpha), CKB (Creatine kinase B-type), and YWHAG (14-3-3 protein gamma) in plasma. As shown in the grouped scatter plot in **Figure 3**, there was a significant difference in the plasma level of CAMK2A between the R and S group (R: 29 vs S: 38, P=0.0074). The CAMK2A level was significantly up-regulated in the R group, which was consistent with the TMT quantification result in the proteomic analysis. Two additional proteins, CKB (R: 16 vs S: 21) and YWHAG (R: 33 vs S: 33) has expres-

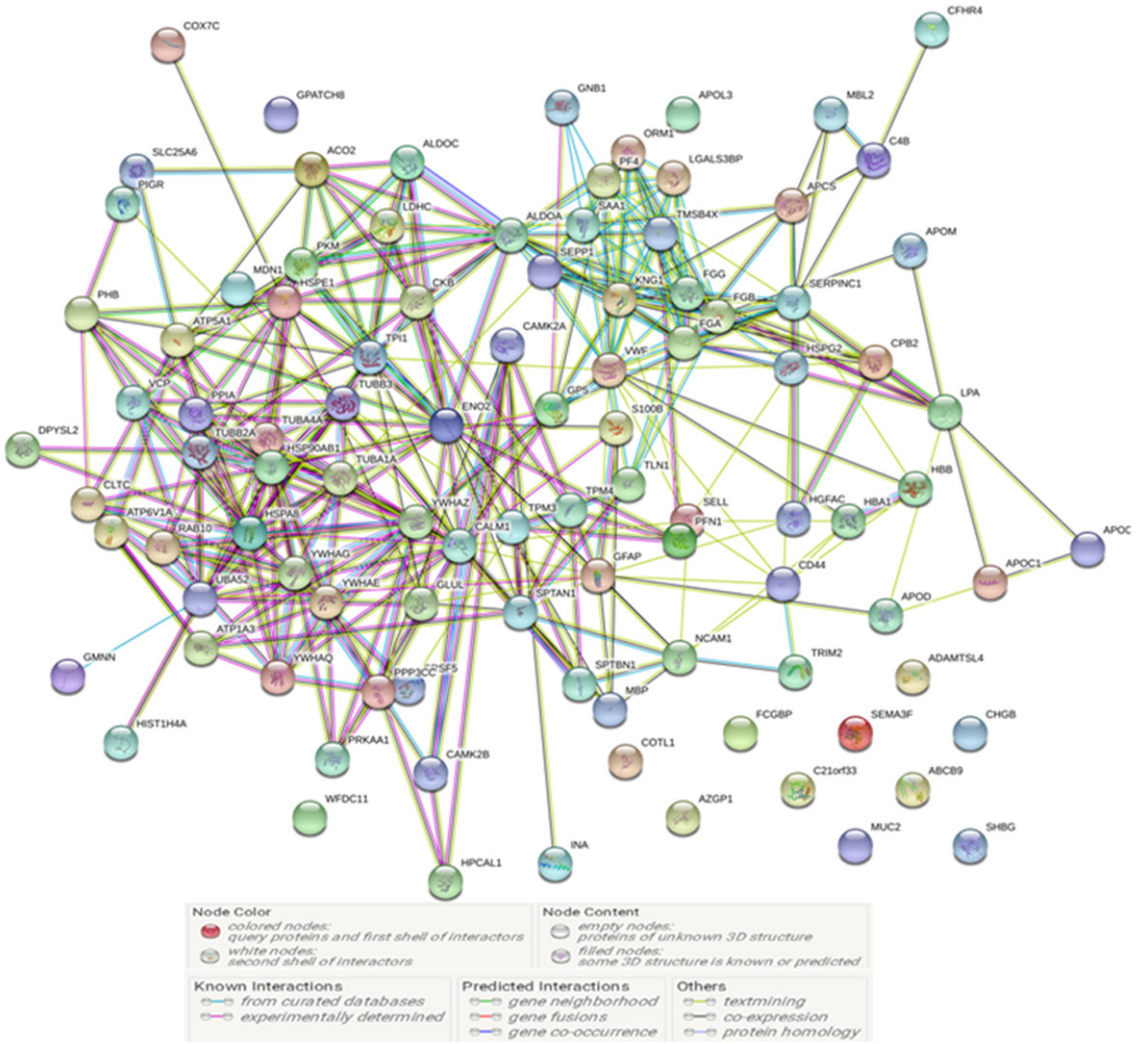

Figure 2. The protein-protein interaction network constructed from the 108 dysregulated proteins using the online tool STRING v10.5. Each edge represents a type of interaction between the linked nodes.

sion levels that were also up-regulated in the R group, consistent with the proteomics results. However, the difference was not statistically significant (P>0.05). Furthermore, the ROC curve analysis showed that AUC was 0.708 for CAMK2A, 0.596 for CKB, and 0.563 for YWHAG (**Figure 3B**). The sensitivityand specificity of CAMKK2A was 48.4% and 86.1% respectively.

Combination analysis with clinicopathologic factors

The association of CAMK2A and other clinicopathologic factors with chemotherapy response was analyzedwith univariate and multivariate logistic regression methods. The level of plasma CAMK2A was identified as an independent predictive factor for chemotherapeutic response (P=0.009, OR=0.152). The ORR of the patients with higher CAMK2A level was 35.3% and the patients with lower CAMK2A level was 63.6% (**Table 4**). In the Log-Rank analysis, patients with higher CAMK2A level had shorter OS than patients with lower CAMK2A level, which amounted to 13.9 and 28.9 months, respectively (P=0.034). While CAMK2A level had no significant effect on PFS, which was 2.9 and 8.6 months for the patients with higher and lower CAMK2A level (P=0.060) (**Figure 4**). In the multivariate Cox regression analysis, CAMK2A level still had a significant effect on OS (P=0.031, HR=1.865) (**Table 5**).

Table 3. Bioinformatics analysis of the proteomic results

KEGG Pathways				
Pathway ID	Pathway description	Observed gene count	False discovery rate	Matching proteins in your network (labels)
4610	Complement and coagulation cascades	9	1.02E-08	C4B, CPB2, FGA, FGB, FGG, KNG1, MBL2, SERPINC1, VWF
1230	Biosynthesis of amino acids	7	4.18E-06	ACO2, ALDOA, ALDOC, ENO2, GLUL, PKM, TPI1
4114	Oocyte meiosis	8	4.18E-06	CALM1, CAMK2A, CAMK2B, PPP3CC, YWHAE, YWHAG, YWHAQ, YWHAZ
Biological Process (GO)				
Pathway ID	Pathway description	Observed gene count	False discovery rate	Matching proteins in your network (labels)
GO: 0002576	Platelet degranulation	13	2.36E-12	ALDOA, CALM1, FGA, FGB, FGG, KNG1, PF4, PFN1, PPIA, TLN1, TMSB4X, TUBA4A, VWF
GO: 0030168	Platelet activation	17	3.05E-12	ALDOA, CALM1, FGA, FGB, FGG, GNB1, GP5, KNG1, PF4, PFN1, PPIA, SAA1, TLN1, TMSB4X, TUBA4A, VWF, YWHAZ
GO: 0065008	Regulation of biological quality	46	3.05E-12	ALDOA, APCS, APOC4, ATP1A3, ATP6V1A, AZGP1, CALM1, CAMK2A, CAMK2B, CD44, CKB, CPB2, DPYSL2, FGA, FGB, FGG, GFAP, GLUL, GP5, HIST1H4A, HSP90AB1, HSPA8, KNG1, LPA, MBL2, MUC2, PF4, PFN1, PHB, PIGR, PPIA, PRKAA1, S100B, SAA1, SELL, SEMA3F, SERPINC1, SLC25A6, SPTAN1, SPTBN1, TLN1, TUBA4A, VWF, YWHAE, YWHAG, YWHAZ
GO: 0009611	Response to wounding	25	7.82E-12	ALDOA, APOD, CALM1, CPB2, FGA, FGB, FGG, GFAP, GNB1, GP5, KNG1, LPA, PF4, PFN1, PKM, PPIA, SAA1, SELL, SERPINC1, SRSF5, TLN1, TMSB4X, TUBA4A, VWF, YWHAZ
GO: 0007596	Blood coagulation	21	4.52E-11	ALDOA, CALM1, CD44, CPB2, FGA, FGB, FGG, GNB1, GP5, KNG1, PF4, PFN1, PPIA, SAA1, SELL, SERPINC1, TLN1, TMSB4X, TUBA4A, VWF, YWHAZ
Molecular Function (GO)				
Pathway ID	Pathway description	Observed gene count	False discovery rate	Matching proteins in your network (labels)
GO: 0005515	Protein binding	53	2.07E-09	ABCB9, ADAMTSL4, ALDOA, ALDOC, APCS, ATP1A3, ATP5A1, AZGP1, CALM1, CAMK2A, CAMK2B, CD44, CHGB, CKB, CLTC, COTL1, FGB, FGG, GLUL, GMNN, GNB1, HBB, HIST1H4A, HSP90AB1, HSPA8, HSPE1, HSPG2, KNG1, LPA, MBL2, MDN1, NCAM1, PF4, PFN1, PHB, PKM, PPIA, RAB10, S100B, SAA1, SELL, SERPINC1, SPTAN1, SPTBN1, TLN1, TPI1, UBA52, VCP, VWF, YWHAE, YWHAG, YWHAQ, YWHAZ
GO: 0005200	Structural constituent of cytoskeleton	9	1.90E-06	GFAP, INA, SPTAN1, SPTBN1, TLN1, TUBA1A, TUBA4A, TUBB2A, TUBB3
GO: 0005198	Structural molecule activity	15	7.19E-05	CLTC, FGA, FGB, FGG, GFAP, INA, MBP, SPTAN1, SPTBN1, TLN1, TPM4, TUBA1A, TUBA4A, TUBB2A, TUBB3
GO: 0097367	Carbohydrate derivative binding	29	9.76E-05	ABCB9, ATP1A3, ATP5A1, ATP6V1A, AZGP1, CAMK2A, CAMK2B, CD44, CKB, GLUL, HSP90AB1, HSPA8, HSPE1, KNG1, LPA, MDN1, PF4, PKM, PRKAA1, RAB10, SAA1, SELL, SERPINC1, TUBA1A, TUBA4A, TUBB2A, TUBB3, VCP, VWF
GO: 0023026	MHC class II protein complex binding	4	0.000131	HSP90AB1, HSPA8, PKM, YWHAE
Cellular Component (GO)				
Pathway ID	Pathway description	Observed gene count	False discovery rate	Matching proteins in your network (labels)
GO. 0044421	Extracellular region part	69	1.93E-28	ADAMTSL4, ALDOA, ALDOC, APCS, APOC1, APOC4, APOD, ATP1A3, ATP5A1, ATP6V1A, AZGP1, CALM1, CD44, CKB, CLTC, COTL1, CPB2, DPYSL2, ENO2, FCGBP, FGA, FGB, FGG, GLUL, GNB1, GP5, HBA1, HGFAC, HIST1H4A, HPCAL1, HSP90AB1, HSPA8, HSPE1, INA, KNG1, LDHC, LGALS3BP, LPA, MBL2, MUC2, NCAM1, ORM1, PF4, PFN1, PHB, PIGR, PKM, PPIA, PPP3CC, RAB10, S100B, SAA1, SEMA3F, SERPINC1, SHBG, SPTAN1, SPTBN1, TLN1, TPM3, TUBA1A, TUBA4A, TUBB2A, TUBB3, VCP, VWF, YWHAE, YWHAG, YWHAQ, YWHAZ
GO. 1903561	Extracellular vesicle	61	1.82E-27	ALDOA, ALDOC, APCS, APOC1, APOD, ATP1A3, ATP5A1, ATP6V1A, AZGP1, CALM1, CD44, CKB, CLTC, COTL1, CPB2, DPYSL2, ENO2, FCGBP, FGA, FGB, FGG, GLUL, GNB1, GP5, HBA1, HIST1H4A, HPCAL1, HSP90AB1, HSPA8, HSPE1, HSPG2, KNG1, LDHC, LGALS3BP, NCAM1, ORM1, PFN1, PHB, PIGR, PKM, PPIA, PPP3CC, RAB10, SAA1, SEPP1, SERPINC1, SHBG, SPTAN1, SPTBN1, TLN1, TPM3, TUBA1A, TUBA4A, TUBB2A, TUBB3, VCP, VWF, YWHAE, YWHAG, YWHAQ, YWHAZ

GO. 0005576	Extracellular region	72	2.11E-27	ADAMTSL4, ALDOA, ALDOC, APCS, APOC1, APOC4, APOD, APOL3, ATP1A3, ATP5A1, ATP6V1A, AZGP1, CALM1, CD44, CFHR4, CHGB, CKB, CLTC, COTL1, CPB2, DPYSL2, ENO2, FCGBP, FGA, FGB, FGG, GLUL, GNB1, GP5, HBA1, HIST1H4A, HPCAL1, HSP90AB1, HSPA8, HSPE1, INA, KNG1, LDHC, LGALS3BP, LPA, MBL2, MUC2, NCAM1, ORM1, PF4, PFN1, PHB, PIGR, PKM, PPIA, PPP3CC, RAB10, SAA1, SEMA3F, SERPINC1, SHBG, SPTAN1, SPTBN1, TLN1, TMSB4X, TPM3, TUBA1A, TUBA4A, TUBB2A, TUBB3, VCP, VWF, WFDC11, YWHAE, YWHAG, YWHAQ, YWHAZ
GO. 0070062	Extracellular exosome	60	8.03E-27	ALDOA, ALDOC, APCS, APOC1, APOD, ATP5A1, ATP6V1A, AZGP1, CALM1, CD44, CKB, CLTC, COTL1, CPB2, DPYSL2, ENO2, FCGBP, FGA, FGB, FGG, GLUL, GNB1, GP5, HBA1, HIST1H4A, HPCAL1, HSP90AB1, HSPA8, HSPE1, HSPG2, KNG1, LDHC, LGALS3BP, NCAM1, ORM1, PFN1, PHB, PIGR, PKM, PPIA, PPP3CC, RAB10, SAA1, SEPP1, SERPINC1, SHBG, SPTAN1, SPTBN1, TLN1, TPM3, TUBA1A, TUBA4A, TUBB2A, TUBB3, VCP, VWF, YWHAE, YWHAG, YWHAQ, YWHAZ
GO. 0031988	Membrane-bounded vesicle	64	7.84E-26	ALDOA, ALDOC, APCS, APOC1, APOD, ATP5A1, ATP6V1A, AZGP1, CALM1, CAMK2A, CAMK2B, CD44, CHGB, CKB, COTL1, CPB2, DPYSL2, ENO2, FCGBP, FGA, FGB, FGG, GLUL, GNB1, GP5, HBA1, HIST1H4A, HPCAL1, HSP90AB1, HSPA8, HSPE1, HSPG2, KNG1, LDHC, LGALS3BP, NCAM1, ORM1, PF4, PFN1, PHB, PIGR, PKM, PPIA, PPP3CC, RAB10, SAA1, SEPP1, SERPINC1, SHBG, SPTAN1, SPTBN1, TLN1, TMSB4X, TPM3, TUBA1A, TUBA4A, TUBB2A, TUBB3, VCP, VWF, YWHAE, YWHAG, YWHAQ, YWHAZ

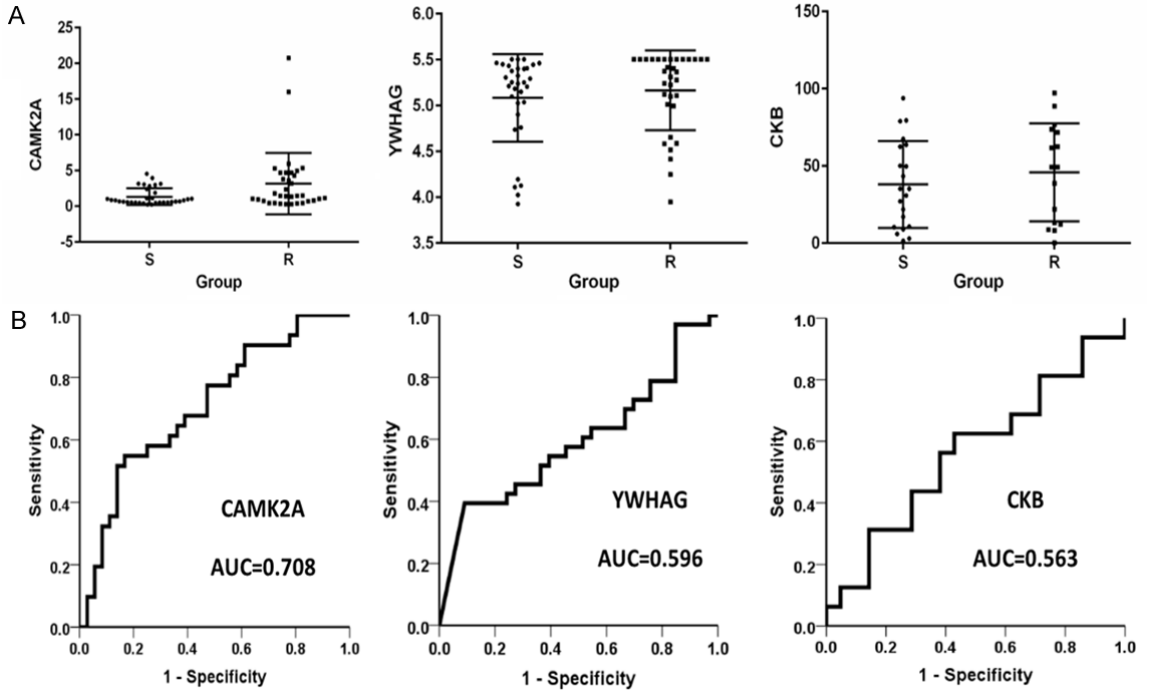

Figure 3. The ELISA test result and ROC analysis of CAMK2A, CKB, and YWHAG in 67 plasma samples. R: resistance group. S: sensitive group.

Discussion

Quantitative proteomics is driving the discovery of disease-specific targets and biomarkers. UHPLC and mass spectrometry-based proteomics were combined with TMT labeled samples to quantify protein expression changes. Due to its faster separation,greater sensitivity, and resolution, we applied the TMT-based proteomic approach to discover and identify plasma protein biomarkers for predicting docetaxel-basedchemoresistance in the metastatic TNBC patients.

In this study, we found 108 differently expressed proteins which demonstrated at least a 1.3-fold difference between the R and S group withMT-based proteomic approach. Furthermore, we selected 3 proteins (CKB, YWHAG (isoform of 14-3-3 gamma) and CAMKIIA) for further valida-

Table 4. The correlation of CAMK2A and other clinicopathologic factors with chemotherapy response rate

Characteristics		ORR (%)	Single variate	Multivariate	
			P	*P*	OR
Age	≤53	44.1	0.393	0.811	1.180
	>53	54.5			
ECOG	0, 1	50.8	0.614*	0.999	0.001
	2	25.0			
Grading	G1	50.0	0.927	0.432	1.656
	G2-3	48.8			
AJCC stage at diagnosis	Stage I-III	51.7	0.672*	0.277	3.531
	Stage IV	40.0			
Internalorgan metastasis (liver, lung, brain)	Yes	50.0	0.866	0.897	0.906
	No	47.8			
Sites of metastasis ≥3	Yes	48.6	0.912	0.521	1.200
	No	50.0			
CAMK2A	High	35.3	0.02	0.009	0.152
	Low	63.6			

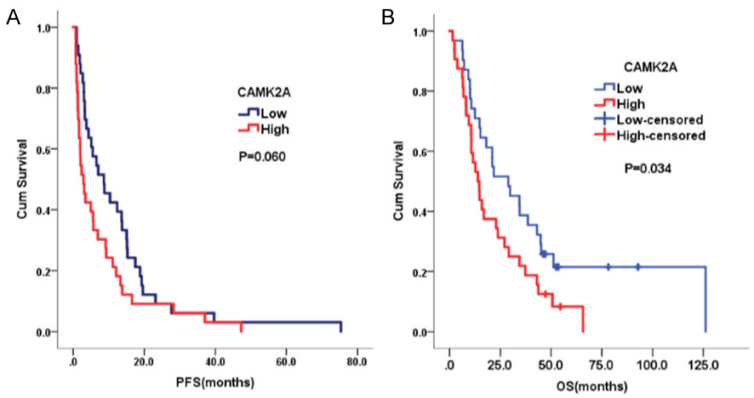

Figure 4. The progression free survival (PFS) and overall survival (OS) of patients with high and low CAMK2A in plasma.

tion. The 4 isoforms of 14-3-3 (epsilon, gamma, theta/tauand zeta/delta) which were upregulated in the R group.The association between chemotherapy resistance in breast cancer and expression of 14-3-3 proteins has been reported previously [10, 14-16]. There are seven isoforms of 14-3-3 (beta/alpha, epsilon, gamma, eta, theta/tau, sigma/stratifin and zeta/delta), which are reported to associate with proteins involved in critical processes including cell cycle regulation, intracellular signaling, and apoptosis [17]. Due to the nature of their protein targets, 14-3-3 proteins have been widely associated with cancer, including response to therapeutic agents and it is thought that 14-3-3 proteins promote cell survival by inhibition of apoptosis [18]. In the current study, ELISA assays demonstrated that the expression levels of CKBand YWHAG (isoform of 14-3-3 gamma) were up-regulated in the R group, consistent with the proteomics results. However, the difference was not statistically significant (*P*>0.05). Calcium/calmodulin-dependent protein kinase (CAMK) is a large family of protein kinases that act as an effector of calcium/calmodulin, which have been classified into myosin light chain kinase, phosphorylase kinase, CAM kinase I, CAM kinase II, EF-2 kinase (CAM kinase III) and CAM kinase IV [19]. Calcium/calmodulin-dependent protein kinase II (CAMKII) is a multifunctional calcium/calmodulin-dependent serine/threonine protein kinase. Recent studies suggest that CaMKII plays important roles in the control of cell cycle progression and cell proliferation [20-22]. Potential connections between $Ca2^{+}$/CaMKII signaling and multiple signaling pathways have been reported in many cell types. Runbi et al [23] found that mesenchymal stem cell (MSC)-exosomes potentiated chemoresistance in gastric cancer cells *in vivo* and *ex vivo* and exerted

Table 5. The correlation of CAMK2A and other clinicopathologic factors with overall survival

Characteristics		OS (median)	Log-rank	Cox Regression	
			P	*P*	HR
Age	≤53	14.7	0.078	0.508	0.771
	>53	22.9			
ECOG	0, 1	21.0	0.07	0.007	4.499
	2	2.4			
Grading	G1	29.2	0.504	0.797	1.085
	G2-3	14.7			
AJCC stage at diagnosis	Stage I-III	16.9	0.182	0.218	2.526
	Stage IV	14.8			
Internal organ metastasis (liver, lung, brain)	Yes	15.9	0.081	0.368	1.484
	No	21.8			
Sites of metastasis ≥3	Yes	14.8	0.046	0.409	1.349
	No	22.9			
CAMK2A	High	13.9	0.034	0.031	1.865
	Low	28.9			

this role at least in part through the activation of CAMKs (predominantly CAMKII and CAMKIV) and the downstream Raf/MEK/ ERK pathway. The tumor microenvironment is emerging as a significant determinant of a tumor's response to chemotherapy [24, 25] and MSCs have been considered as an important component of the tumor microenvironment. The Raf/MEK/ERK kinase cascade is one of the downstream pathways of the CAMKs.

In our study, the CAMKIIA level was significantly up-regulated in the R group, which is consistent with the TMT quantification result in the proteomic analysis. Furthermore, the ROC curve analysis showed that the AUC was 0.708 for CAMK2A, 0.596 for CKB and 0.563 for YWHAG (**Figure 3B**). These data indicate that CAMK2A could be potential biomarker to distinguish the R group from the S group of metastatic TNBC patientswith high sensitivity and specificity. When tested for its ability to predict PFS and OS, the median value of the CAMK2A level separated patients into significantly different groups, those with values above the median showing significantly shorter OS than those with values below the median.

Docetaxel is one of the common drugs used to treat metastatic breast cancer which binds to β-tubulin in assembled tubulin, thereby reducing depolymerisation [26]. Chemoresistance is a major factor involved in poor response and reduced overall survival in patients with locally advanced and metastatic breast cancer. Chemoresistance is a very challenging and complex phenomenon involving a number of complex mechanisms. The most established *in vitro* mechanism for resistance is overexpression of drug efflux proteins. The best known drug efflux proteins are members of the ATP-binding cassette (ABC) superfamily, including P-glycoprotein (Pgp), multidrug resistance associated protein 1 (MRP-1), and breast cancer resistance protein (BCRP), which export anticancer agents out of cells [27, 28]. However, the results in clinical studies are controversial. Some studies showed no correlation between ABC transporter expression level and response to either paclitaxel or docetaxel treatment in breast cancer patients [29].

This study has some limitations. First, the samples of the study were limited and a larger number of patients are required to confirm the prognostic significance. Second, the data were retrospectively collected from prospectively maintained database. Third, we did not explore all the dysregulated proteins identified in the proteomics analysis. The combination of proteins might have been more predictive.

In summary, using a TMT-Based Proteomics Analysis of plasma samples, we were able to identify differentially expressed proteins predictive of chemotherapy resistance in the met-

astatic TNBC. The plasma CAMK2A level may serve as apotential predictive and prognosis biomarker for chemotherapy and deserves further prospective trials for validation.

Acknowledgements

This work was supported in part by grant from the National Natural Science Foundation of China (No. 81160214) and Beijing Natural Science Foundation of China (No. 7143173).

Disclosure of conflict of interest

None.

Address correspondence to: Huiping Li, Key Laboratory of Carcinogenesis and Translational Research (Ministry of Education/Beijing), Department of Medical Oncology, Peking University Cancer Hospital & Institute, Beijing 100142, P.R. China. E-mail: huipingli2012@hotmail.com; Jing Shen, Key Laboratory of Carcinogenesis and Translational Research (Ministry of Education/Beijing), Central Laboratory, Peking University Cancer Hospital & Institute, Beijing 100142, P.R. China. E-mail: shenjing@bjmu.edu.cn

References

[1] Siegel RL, Miller KD, Jemal A. Cancer statistics, 2017. CA Cancer J Clin 2017; 67: 7-30.

[2] Zheng R, Zeng H, Zhang S, Chen T, Chen W. National estimates of cancer prevalence in China, 2011. Cancer Lett 2016; 370: 33-38.

[3] Early Breast Cancer Trialists' Collaborative Group. Effects of chemotherapy and hormonal therapy for early breast cancer on recurrence and 15-year survival: an overview of the randomised trials. Lancet 2005; 365: 1687-1717.

[4] Schneider AP 2nd, Zainer CM, Kubat CK, Mullen NK, Windisch AK. The breast cancer epidemic: 10 facts. Linacre Q 2014; 81: 244-277.

[5] Opstal-van Winden AW, Vermeulen RC, Peeters PH, Beijnen JH, van Gils CH. Early diagnostic protein biomarkers for breast cancer: how far have we come? Breast Cancer Res Treat 2012; 134: 1-12.

[6] Bohm D, Keller K, Wehrwein N, Lebrecht A, Schmidt M, Kölbl H, Grus FH. Serum proteome profiling of primary breast cancer indicates a specific biomarker profile. Oncol Rep 2011; 26: 1051-1056.

[7] Lei L, Wang XJ, Zheng ZG, Huang J, Cao WM, Chen ZH, Shao XY, Cai JF, Ye WW, Lu HY. Identification of serum protein markers for breast cancer relapse with SELDI-TOF MS. Anat Rec (Hoboken) 2011; 294: 941-944.

[8] Duffy MJ. Serum tumor markers in breast cancer: are they of clinical value? Clin Chem 2006; 52: 345-351.

[9] Hanash SM, Pitteri SJ, Faca VM. Mining the plasma proteome for cancer biomarkers. Nature 2008; 452: 571-579.

[10] Chuthapisith S, Layfield R, Kerr ID, Hughes C, Eremin O. Proteomic profiling of MCF-7 breast cancer cells with chemoresistance to different types of anti-cancer drugs. Int J Oncol 2007; 30: 1545-1551.

[11] Aebersold R, Mann M. Mass spectrometry-based proteomics. Nature 2003; 422: 198-207.

[12] Yates JR 3rd, Gilchrist A, Howell KE, Bergeron JJ. Proteomics of organelles and large cellular structures. Nat Rev Mol Cell Biol 2005; 6: 702-714.

[13] Walther TC, Mann M. Mass spectrometry-based proteomics in cell biology. J Cell Biol 2010; 190: 491-500.

[14] Hodgkinson VC, ELFadl D, Agarwal V, Garimella V, Russell C, Long ED, Fox JN, McManus PL, Mahapatra TK, Kneeshaw PJ, Drew PJ, Lind MJ, Cawkwell L. Proteomic identification of predictive biomarkers of resistance to neoadjuvant chemotherapy in luminal breast cancer: a possible role for 14-3-3 theta/tau and tBID? J Proteomics 2012; 75: 1276-1283.

[15] Hodgkinson VC, Eagle GL, Drew PJ, Lind MJ, Cawkwell L. Biomarkers of chemotherapy resistance in breast cancer identified by proteomics: current status. Cancer Lett 2010; 294: 13-24.

[16] Liu Y, Liu H, Han B, Zhang JT. Identification of 14-3-3sigma as a contributor to drug resistance in human breast cancer cells using functional proteomic analysis. Cancer Res 2006; 66: 3248-3255.

[17] Tzivion G, Gupta VS, Kaplun L, Balan V. 14-3-3 proteins as potential oncogenes. Semin Cancer Biol 2006; 16: 203-213.

[18] Masters SC, Subramanian RR, Truong A, Yang H, Fujii K, Zhang H, Fu H. Survival-promoting functions of 14-3-3 proteins. Biochem Soc Trans 2002; 30: 360-365.

[19] Nairn AC, Picciotto MR. Calcium/calmodulin-dependent protein kinases. Semin Cancer Biol 1994; 5: 295-303.

[20] Ducibella T, Schultz RM, Ozil JP. Role of calcium signals in early development. Semin Cell Dev Biol 2006; 17: 324-32.

[21] Zayzafoon M. Calcium/calmodulin signaling controls osteoblast growth and differentiation. J Cell Biochem 2006; 97: 56-70.

[22] Colomer J, Means AR. Physiological roles of the Ca2+/CaM-dependent protein kinase cascade in health and disease. Subcell Biochem 2007; 45: 169-214.

[23] Ji R, Zhang B, Zhang X, Xue J, Yuan X, Yan Y, Wang M, Zhu W, Qian H, Xu W. Exosomes derived from human mesenchymal stem cells confer drug resistance in gastric cancer. Cell Cycle 2015; 14: 2473-2483.
[24] Chien J, Kuang R, Landen C, Shridhar V. Platinum-sensitive recurrence in ovarian cancer: the role of tumor microenvironment. Front Oncol 2013; 3: 251.
[25] Mao Y, Keller ET, Garfield DH, Shen K, Wang J. Stromal cells in tumor microenvironment and breast cancer. Cancer Metastasis Rev 2013; 32: 303-315.
[26] Jordan MA, Wilson L. Microtubules as a target for anticancer drugs. Nat Rev Cancer 2004; 4: 253-265.
[27] McGrogan BT, Gilmartin B, Carney DN, McCann A. Taxanes, microtubules and chemoresistant breast cancer. Biochim Biophys Acta 2008; 1785: 96-132.
[28] Zelnak A. Overcoming taxane and anthracycline resistance. Breast J 2010; 16: 309-312.
[29] Kanzaki A, Toi M, Nakayama K, Bando H, Mutoh M, Uchida T, Fukumoto M, Takebayashi Y. Expression of multidrug resistance-related transporters in human breast carcinoma. Jpn J Cancer Res 2001; 92: 452-458.